Proc. Natl. Acad. Sci. USA
Vol. 86, pp. 9626–9630, December 1989
Population Biology

Ordered appearance of antigenic variants of African trypanosomes explained in a mathematical model based on a stochastic switch process and immune-selection against putative switch intermediates

(variant surface glycoprotein/parasitemia/antibody-mediated killing/antigenic variation/differential equations)

Z. AGUR*†, D. ABIRI*, AND L. H. T. VAN DER PLOEG‡

*Department of Applied Mathematics, The Weizmann Institute of Science, Rehovot 76100, Israel; and ‡Department of Genetics and Development, College of Physicians and Surgeons, Columbia University, New York, NY 10032

Communicated by William Trager, July 21, 1989 (received for review February 2, 1989)

ABSTRACT **Antigenic variation of African trypanosomes results from the periodic activation of a single new variant cell surface glycoprotein (VSG) gene out of a repertoire of about a 1000 VSG genes. In spite of the apparently random genetic basis of the process of antigenic variation, the relapsing parasitemias are characterized by an as yet unexplained order of appearance of major VSG variants. Here we mathematically test hypotheses concerning the blood-based parasitemia. In our model the antigenic switches occur at random at the DNA level. A variable proportion of the switches has a short intermediate phase in which two different VSGs simultaneously occur on the cell surface. We show that, in a theoretical population of 230 single expressor variants in an immunocompetent or in an immunodeficient host, it is *not* possible to explain the ordered appearance of variants by affecting the growth coefficients of single expressors or double expressors or by affecting the antigen switch probabilities. Rather, a realistic parasitemia can be obtained if the majority of switches has a double expressor switch-intermediate phase and if the double expressors have a differential susceptibility to the immune control. This study is significant in providing a theoretical basis for the ordered appearance of variants and in explaining previously unresolved discrepancies between the rate of appearance of new variants in culture and *in vivo*. In addition, testable predictions as to the development of the infections, switch rate of variants, fraction of double expressors, and parasite mortality coefficients are generated.**

African trypanosomes, exemplified by *Trypanosoma brucei*, the causative agent of sleeping sickness, escape immunodestruction through the periodic generation of a few daughter cells in which the antigenic composition of the cell surface coat is entirely altered (1–3). This cell surface coat consists of densely packed identical variant cell surface glycoprotein (VSG) molecules. Each VSG coat results from the transcription of a single VSG gene. The repertoire of individual VSG coats is extensive since there are ≈1000 different VSG genes (4). Parasitemias are characterized by a gradual increase in the number of parasites expressing a particular VSG, followed by specific antibody-mediated decimation (4–7). This population is then replaced by the next VSG-specific parasite population (8–10).

VSG genes can be sequentially activated through one of two different mechanisms. In the first mechanism, a silent or basic copy VSG gene displaces the previously active VSG gene, located in a VSG gene expression site. This DNA recombinational process resembles the unidirectional gene conversion of the yeast mating type switches (11). In the second mechanism, antigenic switches result from differential transcriptional control of the expression sites (for review, see ref. 11). Trypanosomes usually express only a single VSG gene. However, expression of more than one VSG gene at a time was proposed to exist following the discovery of trypanosomes with a mixed (double) coat (12). Molecular genetical analysis of VSG gene expression identified a trypanosome with a double coat resulting from two different simultaneously active VSG gene expression sites (13). Further evidence for double coats came from the isolation of a trypanosome with two simultaneously active VSG gene expression sites, only one of which produced VSG mRNA (14). The existence of "doubly expressing" trypanosomes (DEs) lead to the proposal that these might represent intermediates in the process of coat switching whether it occurs through gene displacement or through differential transcriptional control of expression sites (15, 16).

In spite of preliminary evidence suggesting that VSG gene switching is a random process (14, 15, 17) antigenic variants arise in an imprecise order (18, 19), with a population of a particular variant resulting from multiple (up to 10) independent activations of the same VSG gene (15–17). There is no evidence for a DNA-mediated control mechanism explaining multiple independent activations and the ordered occurrence of variants (15, 17). An alternative explanation has been proposed, based on immunological selection against certain trypanosomes, in combination with growth competition (for a summary, see refs. 15, 17, 19, 20). These assumptions will be tested to determine whether they can explain the characteristic relapsing parasitemia patterns.

THEORETICAL METHODS

Whereas laboratory experiments and field observations are indispensable for understanding the details of a parasitemia, the *in vivo* dynamics appears too complicated to be *intuitively* inferred from these observations. For a complete understanding of a parasitemia, the interaction of the genetic process leading to antigenic variation, the dynamics of the continuously evolving parasite population, and the immune response have to be formally described and systematically analyzed in concert. In this work we construct a mathematical model that includes the main processes underlying the *in vivo* dynamics of trypanosomiasis. By modulating parameter values, we test assumptions concerning the factors that generate the ordered appearance of dominant variants.

Kosinski (21) presents a model of antigenic variation in trypanosomes, which accounts for the internal dynamics of parasite populations within a single host, for the dynamics of the B-cell population, and for the interaction between the

The publication costs of this article were defrayed in part by page charge payment. This article must therefore be hereby marked "*advertisement*" in accordance with 18 U.S.C. §1734 solely to indicate this fact.

Abbreviations: VSG, variant surface glycoprotein; DE, double expressor; SE, single expressor.

†To whom reprint requests should be addressed.

two. In Kosinski's model every antigenic switch is an event in which a trypanosome with coat "A" converts into a trypanosome with coat "B," without a DE "AB" switch intermediate. Kosinski's analysis shows that differences in the intrinsic growth coefficients of single expressors (SEs) cannot generate the observed ordered parasitemias. A simpler model, proposed by Herbert (22), also failed to explain the dynamics of parasitemia.

We add our assumptions concerning DEs as facultative or obligatory switch intermediates (Eq. 2)§ to Kosinski's model (Eqs. 1, 3, and 4 below). DEs are expected to be of two different types, since they can result from an antigenic switch due to a gene replacement or from an antigenic switch due to the activation of a new and the inactivation of the old expression site. The life span of both types of DE is here for simplicity assumed to be the same. Our numerical study will focus on the characteristic parameters of the DE, using parameters measured experimentally when available.

Assumptions About the Underlying Processes. Our model assumes a serodeme of 230 SE variants (numbered 0–229). Infection is initiated by one SE variant population—variant 0. Each SE variant population grows according to Eq. 1:

$$\frac{dv_n}{dt} = v_n\left[r_n\left(1 - \frac{V}{K}\right) - ua_n\right], \qquad [1]$$

where v_n = population size of variant n; r_n = SE variant-specific intrinsic growth coefficient; V = total parasite population in blood; K = carrying capacity of the host in terms of maximum parasitemia per ml; u = antibody-specific mortality coefficient; and a_n = population size of anti-VSG n antibodies (in arbitrary units).

We assume that indirect switches (i.e., requiring a DE intermediate) can be either facultative ($P_{DE} < 1$) or obligatory ($P_{DE} = 1$). No symmetry is assumed in our model—i.e., growth parameters of variant n,m are not necessarily identical to those of variant m,n. Hence, the potential number of DE variants is $230 \times 230 - 230 = 52{,}670$. SE to SE, or SE to DE and DE to SE transitions are taken as completely random events, occurring with constant, nonspecific, probabilities $P_{n\to m}$, $P_{n\to n,m}$, and $P_{n,m\to m}$, respectively. The population size of a particular DE, which simultaneously expresses VSGs n and m, is denoted by $v_{n,m}$, indicating that VSG m is preceded by VSG n. As the DEs expose two distinct VSGs, we assume that their growth is affected by antibodies to both these molecules:

$$\frac{dv_{n,m}}{dt} = v_{n,m}\left[r_{n,m}\left(1 - \frac{V}{K}\right) - (u'_{n,m}a_n + u''_{n,m}a_m)\right], \qquad [2]$$

where $u'_{n,m}$ and $u''_{n,m}$ are the mortality coefficients of DE n,m due to anti-n and anti-m antibodies, respectively. As DEs in chronic infections do not occur in the blood in detectable numbers (12, 13, 23), we assume them to have a negligible effect on B-cell proliferation and antibody secretion. Initially the host carries one B cell for each SE variant, which proliferates upon antigenic stimulation by the parasite:

$$\frac{db_n}{dt} = r_B b_n\left[\frac{v_n}{v_n + C}\right], \qquad [3]$$

where b_n = population size of B cells specific to VSG n; r_B = B-cell intrinsic growth coefficient; and C = size of variant n population at which B cells proliferate at half their maximal rate. C is taken as constant for all n.

§Abiri, D. & Agur, Z., Third Mediterranean Conference on Parasitology, August 4–7, 1987, Jerusalem, abstr. 76.

No removal of B cells is assumed. Thus, the size of the specific B-cell population is a nondecreasing function, allowing for a quick response to future challenges by a reappearing variant. Note, however, that relaxation of this assumption may only bring about a reoccurrence of early variants later in the infection but otherwise does not affect the results. Specific antibodies are secreted as a function of the specific B-cell population size:

$$\frac{da_n}{dt} = c_1 b_n\left[\frac{v_n}{v_n + C}\right] - c_2 a_n, \qquad [4]$$

where c_1 = antibody secretion coefficient; and c_2 = antibody removal coefficient. Here it is assumed for simplicity that removal of antibodies due to specific antigen binding has a negligible effect on the general antibody numbers (21). However, this assumption should be further investigated.

Only one, spatially homogeneous, growth site is assumed in our work—the blood. Thus we do not take into account the potential effects of parasites that might be sequestered in other tissues. Our model shows that with a few testable assumptions the course of a blood-based parasitemia can be explained. However, it cannot exclude the possibility that other factors, like repopulation of the blood by trypanosomes that occupy intracellular sites (10), may also affect the dynamics.

Assumptions About Parameter Values. Parameter ranges used in the simulations of the model are summarized in Tables 1 and 2. We assume that the population doubling time (*PDT*) ranges from 5 hr, for the fastest growing variant 0, to 15.5 hr, for the slowest growing variant 229. This assumption is based on measurements ranging from 5 hr *in vivo* (24) to 8–15 hr *in vitro* (25). The resulting growth coefficient, r_n, is calculated by the following arbitrary function:

$$r_n = 0.995^n \times PDT(0)^{-1} \times T \times \ln 2, \qquad [5]$$

where $PDT(0)$ is the *PDT* of variant 0; and T is the factor (in time units) that adjusts r_n to the integration time unit of Eqs. 1–4 (6 hr). Blood volume is taken to be 5 liters, suggesting a naturally infected large animal. The carrying capacity assumed here, 5×10^8 per ml and 5×10^{10} per ml, is in accordance with previous estimations (21, 24). A host detection threshold is assumed, 10 parasites per ml; when a variant population grows above this threshold, specific B-cell proliferation begins. We also assume that specific antibody

Table 1. Assumptions about parameter ranges

Parameter	Range of simulated values
Potential number of SE variants	230
Potential number of DE variants	52,670
r_n	0.268–0.85
$r_{n,m}$	0.2–0.85
u	5×10^{-6}
$u'_{n,m}$, $u''_{n,m}$	1×10^{-11}–5×10^{-6}
P_{DE}	0.6–1.0
$P_{n\to n,m}$	1×10^{-6}–1×10^{-3} per division
$P_{n,m\to m}$	1×10^{-3}–1×10^{-1} per division
r_B	0.0–0.52
C	25,000
c_1	170
c_2	0.15
Time delay for antibody secretion	3 days
K	5×10^8–5×10^{10} per ml
Blood volume	5 liters
Host detection threshold	10 per ml

Table 2. DE antibody-specific mortality coefficients for the simulations in Fig. 2

DE $(n - m)$	Mortality coefficient $u'_{n,m}$	Mortality coefficient $u''_{n,m}$
−2	1×10^{-9}	1×10^{-9}
−30	6×10^{-9}	1×10^{-7}
−47	1×10^{-6}	1×10^{-6}
−85	5×10^{-10}	3×10^{-8}
−100	1×10^{-11}	7×10^{-7}
Other	5×10^{-6}	5×10^{-6}

The mortality coefficients indicate the efficacy with which antibodies can recognize a particular SE or DE, determining the rate of subsequent removal of the parasite from the system. The sets of DE are denoted by the difference $n - m$ [e.g., −2 denotes DE(1, 3), DE(2, 4) . . .].

secretion starts 3 days after a variant has been detected by the host. For the second challenge by the same variant, specific antibody secretion starts with no time delay. The SE antibody-specific mortality coefficient is of the same order of magnitude as previously assumed (21)—namely, 5×10^{-6}. The DE antibody-specific mortality coefficient is assumed to vary over a very large range, from 1×10^{-11} to 5×10^{-6} (see Tables 1 and 2 for details). In some of the simulations below $u_n = u'_{n,m}$, so that the rate of DE mortality [i.e., the term $v_{n,m}(u'_{n,m}a_n + u''_{n,m}a_m)$ in Eq. 2] is equal to that of the SE for the newly generated DE, where $a_m << a_n$. This mortality rate may increase by orders of magnitude due to an increase in antibody titer against this newly expressed VSG antigen, a_m. For reasons given below we also investigate cases in which the DE mortality coefficients, $u'_{n,m}$ and $u''_{n,m}$, can be a few orders of magnitude lower than the antibody-specific mortality coefficient of the old SE, u_n. The switch probabilities, $P_{n\to n,m}$ and $P_{n,m\to m}$, were chosen arbitrarily but their product is $P_{n\to m} = 1 \times 10^{-6}$ in all of the simulations, a value that is well within the range of the biologically determined parameter [1.4×10^{-7} to 3.5×10^{-6} (18)]. We have investigated the effect on the parasitemia of the intrinsic growth coefficients, the antibody-specific mortality coefficients, and the switch probabilities. Theoretical considerations as well as the analysis in ref. 21 imply that the values of other parameters—e.g., the blood volume as well as the constants K and C—will not have a meaningful effect on the general parasitemia pattern.

RESULTS AND DISCUSSION

Effect of DE Intrinsic Growth Coefficient. Initially we assume that the DE phase is obligatory ($P_{DE} = 1$) and check the hypothesis that the ordered appearance of antigenic variants results from differences in the intrinsic growth coefficient of the DE, $r_{n,m}$. We further assume that the antibody mortality coefficients are similar for all SEs and DEs, so that $u_n = u'_{n,m} = u''_{n,m}$. In the first simulation experiment we test whether the parasitemias can be explained by choosing a higher value for the intrinsic growth coefficient for some DEs (Fig. 1*A*). The intrinsic growth coefficients of all possible DE combinations are chosen so that specific DE combinations only, the series (0, 1), (1, 2), (2, 3) . . . (228, 229), grow faster ($r_{n,m} = 0.6$) than any of the other DEs ($r_{n,m} = 0.4$). The antibody-specific mortality coefficients for every DE are chosen so that $u'_{n,m} = u''_{n,m} = 5 \times 10^{-6}$, whereas the switch probabilities are $P_{n\to n,m} = 1 \times 10^{-3}$ per division and $P_{n,m\to m} = 1 \times 10^{-3}$ per division. As can be seen in Fig. 1*A*, rapid removal of all parasites from the system occurs. The second experiment (Fig. 1*B*) tests whether the rapid extinction of the parasite in the above experiment can be prevented if higher values are assumed for the intrinsic growth coefficient of DE, in combination with a higher DE to SE switch probability: $P_{n,m\to m} = 1 \times 10^{-1}$,

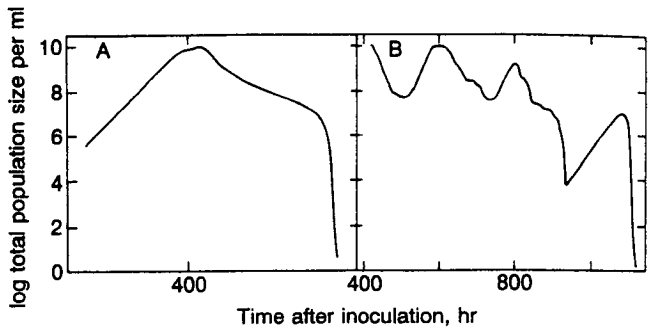

FIG. 1. Simulated parasitemia course for DEs varying in their intrinsic growth coefficients. These simulations are characterized by a simultaneous emergence of many different SE variants. $K = 5 \times 10^8$ per ml; $C = 25{,}000$; $c_1 = 170$; $c_2 = 0.15$; host detection threshold = 10 per ml; $r_B = 0.52$; SE intrinsic growth coefficients vary from $r_n = 0.268$ to $r_n = 0.85$ (see text). (*A*) DE intrinsic growth coefficient is $r_{n,m} = 0.6$ for DE variants (0, 1), (1, 2), (2, 3) . . . (228, 229) and $r_{n,m} = 0.4$ for all other DEs; $u_n = u'_{n,m} = u''_{n,m} = 5 \times 10^{-6}$; $P_{DE} = 1$; $P_{n\to n,m} = 1 \times 10^{-3}$ per division; $P_{n,m\to m} = 1 \times 10^{-3}$ per division. (*B*) $r_{n,m} = 0.85$ for DE (0, 1), (1, 2), (2, 3) . . . (228, 229) and $r_{n,m} = 0.7$ for all other DEs; $u'_{n,m} = u''_{n,m} = 1 \times 10^{-7}$; $P_{n\to n,m} = 1 \times 10^{-5}$ per division; $P_{n,m\to m} = 1 \times 10^{-1}$ per division.

whereas the combined probability $P_{n\to m}$ remains 1×10^{-6}. In addition we reduce the antibody-specific mortality coefficients of the DEs, $u'_{n,m}$ and $u''_{n,m}$ to 1×10^{-7}, leading to an increased survival rate of the DE. The intrinsic growth coefficient of the DE is now $r_{n,m} = 0.85$ for the DE sequence (0, 1), (1, 2), (2, 3) . . . (228, 229), with a lower value ($r_{n,m} = 0.7$) for all other DEs. As can be seen in Fig. 1*B*, increased DE growth coefficients in conjunction with reduced DE antibody-specific mortality coefficients and switch probability, $P_{n,m\to m}$, do not prevent the rapid removal of all parasites from the system. In contrast, simulations of an immunosuppressed host ($r_B = 0$) result in a rapid saturation of the system (results not shown). Still, a mixture of many different SEs is the rule in all of the above experiments, with almost the entire SE repertoire being detected in the system within a time interval of a few days during the peak parasitemia. Further manipulations of the $r_{n,m}$ values and the DE to SE switch probability do not generate a more realistic parasitemia.

Effect of the Host Immune System. Our results indicate that, under the assumption that SEs and DEs only vary in their growth coefficients, infection does not lead to a typical parasitemia with sequential appearance of major variants. We therefore turn to test the hypothesis that it is the interaction between the DE and the immune system that generates the ordered appearance of variants. Hence, in the following simulations each DE has a specific, constant, antibody-mediated mortality coefficient. In contrast to the previous simulations, now the antibody-specific mortality coefficients for the whole population vary over a large range, from 1×10^{-11} to 5×10^{-6} for $u'_{n,m}$ and from 1×10^{-9} to 5×10^{-6} for $u''_{n,m}$ (see Tables 1 and 2 for details). Now $r_{n,m}$ is identical for all DEs. Typical simulation results are shown in Fig. 2*A*, for $P_{DE} = 0.999$, and Table 3, for $P_{DE} = 1$. Fig. 2*A* shows fluctuating parasitemia with each wave corresponding to 1–3 distinct SE major variants (defined as variants whose density exceeds 4500/ml). However, a "cloud" of minor variants, as observed *in vivo*, is always present, although its proportion may go down to about 0.005. The spacing of the maxima in the parasitemia curve is in general agreement with field observations (see window in Fig. 2*A* and refs. 26–28). The exact dependence of the spacing on the temporal parameters of the system should be further investigated. It seems, however, that it can be adjusted—e.g., by manipulating the time delay for specific antibody secretion. Further simulations, for $u''_{n,m} = 5 \times 10^{-6}$ for all DEs, yield similar results.

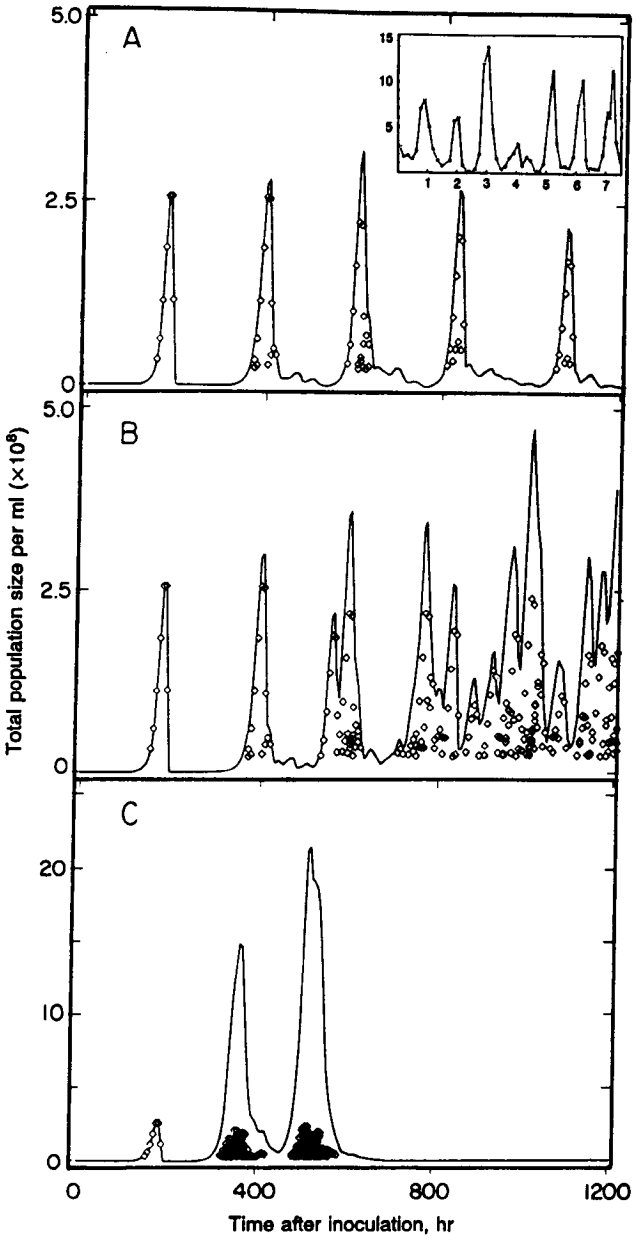

FIG. 2. Simulated parasitemia course for DEs varying in susceptibility to antibody-specific mortality. The population size of each variant exceeding 4500 per ml (a major variant) is marked by a diamond. The total parasite population size is marked by the curved line. $r_{n,m} = 0.2$; $u'_{n,m} = 1 \times 10^{-11}$, 5×10^{-6}; $u''_{n,m} = 1 \times 10^{-9}$, 5×10^{-6} (see Table 2 for details); $K = 5 \times 10^{10}$ per ml; $P_{n,m \to m} = 0.33$ per division; other parameters as in Fig. 1*B*. (*A*) $P_{DE} = 0.999$; here a single major variant constitutes the first peak, whereas two or three major variants constitute the subsequent peaks. A small cloud of minor variants is always present. (*Inset*) Parasitemia curve of a patient under drug treatment. The horizontal axis is time measured in weeks and the vertical axis is number of parasites $\times 10^2$ per ml (ref. 9; redrawn from ref. 8). (*B*) $P_{DE} = 0.995$; here each parasitemic wave corresponds to up to 6 major variants. (*C*) $P_{DE} = 0.90$; here each parasitemic wave corresponds to up to 28 major variants.

Matching major SE variants appearing in Table 3 with their progenitor DE antibody-specific mortality coefficients in Table 2 reveals that a reduction of only half an order of magnitude in $u'_{n,m}$ is enough to make a variant of a dominant early type, even when its intrinsic growth coefficient is relatively low—e.g., variant 47 that emerges from variant 0 (Fig. 3). Thus, a difference in the DE susceptibility to the immune response can explain the parasitemia. In addition, it can easily be envisaged that in the absence of anti-DE antibody-mediated killing, the activation of the alternative complement pathway, or the exposure of common antigenic determinants in coats with gaps, can still give each DE a similar, unique susceptibility to immune control. Therefore, antibody-mediated killing, as well as an incapability of VSGs in DE coats to provide protection, can explain the observed parasitemias. This prediction should be tested in laboratory experiments before further interpretations can be made.

Table 3. First 15 major variants detected in seven simulations for $P_{DE} = 1$

Simulation	Variant														
1	**2**	**30**	**47**	**4**	**87**	**49**	**6**	**62**	**8**	**92**	**64**	**10**	66	**55**	**98**
2	**2**	**47**	**4**	**87**	**60**	**49**	**6**	**62**	**8**	**36**	**64**	**10**	**55**	**68**	**12**
3	**2**	**47**	**4**	**32**	**60**	**6**	**62**	**51**	**8**	**36**	**64**	**92**	**10**	**66**	**68**
4	**2**	**47**	**4**	**32**	**87**	**49**	**6**	**62**	**51**	**8**	**36**	**53**	**93**	**55**	**12**
5	**2**	**30**	**47**	**4**	**87**	**49**	**6**	**62**	**51**	**8**	**36**	**10**	**66**	**55**	**12**
6	**2**	**30**	**47**	**4**	**87**	**49**	**6**	**51**	**36**	**8**	**92**	**53**	**10**	**55**	**12**
7	**2**	**30**	**47**	**4**	**32**	**6**	**51**	**8**	**36**	**64**	**92**	**10**	**98**	**12**	**40**

Here parasitemia is characterized by one wave-specific, major SE variant and regular spacing (9.5 days) between the major peaks. Subsequences appearing in three simulations or more are shown in boldface type. Variant 0, which was used to initiate all simulations, is not shown. For other parameter values, see the legend to Fig. 2.

Effect of the Proportion of Indirect Switches. It may be argued that DEs cannot be responsible for the parasitemia since they are not detected in normal chronic infections. However, in the simulations presented in Table 3, the DE phase is obligatory. Since in these experiments the total DE population is still marginal ($<<10^{-5}$) the data indicate that the DE phase may be obligatory *in vivo* yet exist below our current detection levels. The actual proportion of DEs in the population can be affected by increasing the DE intrinsic growth coefficient so that it becomes equal to that of the average SE ($r_{n,m} = 0.4$ for all DEs). Now DE proportions reach 10^{-5} of the total parasite population. These proportions seem inconsistent with the *in vivo* observations, which predict even lower fractions of DEs. It may therefore be concluded that the intrinsic growth coefficient of the DEs should be lower than that of the SEs. Using similar calculations it can be asserted that SE to DE transition probability should be considerably lower than the DE to SE transition probability. But is an obligatory DE phase a necessary condition for a realistic parasitemia? Our simulations show that parasitemia waves with roughly regular time intervals can be generated only when the proportion of indirect switches is larger than 0.9 (Fig. 2). Moreover, the maximal number of simultaneously detected variants is 34 for $P_{DE} = 0.6$, 28 for $P_{DE} = 0.9$ (Fig. 2*C*), 10 for $P_{DE} = 0.990$, 6 for $P_{DE} = 0.995$ (Fig. 2*B*), 3 for $P_{DE} = 0.999$ (Fig. 2*A*), and 1 for $P_{DE} = 1.0$. These results suggest that indirect antigenic switches play a major role in

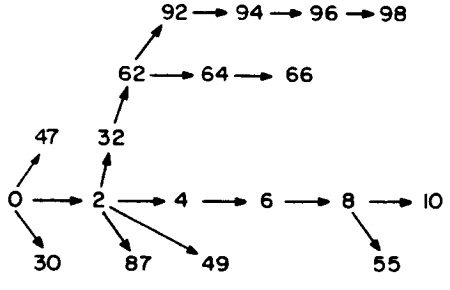

FIG. 3. Full graph of SE variant switches that yielded the major variant sequence appearing in simulation 1 of Table 3. $X \to Y$ indicates that variant X switches to variant Y. Note that variants 32, 94, and 96 in this graph are minor variants and hence are excluded from the presentation of simulation 1 in Table 3. This graph can be retrieved by considering the antibody-mediated mortality coefficients in Table 2.

determining parasitemia patterns in trypanosomiasis. Further empirical data concerning the maximal number of detected variants, the parasitemia peak spacing, and the proportion of DEs can be included in our model for more precise estimates of the proportion of indirect switches, as well as the DE intrinsic growth coefficient, and SE to DE and DE to SE switch probabilities.

Order of Major Variant Emergence. The simulation experiments described above, for P_{DE} tending to unity, are consistent with *in vivo* observations. (*i*) The order of emergence of the major variants in nature has been shown not to correspond to their growth rate (18, 19, 24). Similarly, in our system, the order in which major variants are detected does not correspond to their growth rate. Slower-growing variants (denoted by larger index numbers) can be detected earlier than faster-growing variants (denoted by smaller index numbers) (Table 3). Helped by the values of the DE antibody-specific mortality coefficients in Table 2 one can easily retrieve the graph of SE transitions, including both minor variants and major variants, that yield the major variant sequence in Table 3. From this graph (Fig. 3) it can be concluded that the major variant sequence is primarily determined by the antibody-specific mortality coefficients of the DE and secondarily by the intrinsic growth rate of the SE. An example is given by variant 87, which, due to its lower antibody-specific mortality coefficient, always precedes the faster-growing variant 49. (*ii*) A detailed analysis of the variant sequences in our simulations shows that as many as 11 early variants (not detected after day 60) first appear in the system on exactly the same day in at least three independent simulations (each simulation represents a different individual host taken from the same host population) and 7 late variants (not detected earlier than day 85) appear on the same day in at least three different simulations (Table 3). An important observation seems to be that the majority of variants first appear in the system, though at low levels, within a period of 10 days. (*iii*) As it occurs *in vivo* some highly ordered subsequences are observed in the simulations, such as the sequence 2, 30, 47, 4, 87, 49, 6, which appears in three of the seven simulations, and the sequence 49, 6, 62, which appears in four of the seven simulations (Table 3). It is of interest to note that the order with which variants emerge can be reduced by introducing variation in the DE intrinsic growth rate $r_{n,m}$. Finally, preferential activation of telomeric genes, early in the infection, or a DNA nucleotide sequence controlled preferential activation of some VSG genes (29, 30) are represented in our model by higher switch probabilities for some variants. These variants will preferentially appear in the population, provided that their $u'_{n,m}$ is relatively small. The striking prediction of the model is, however, that even if all switches had similar probabilities an ordered appearance of VSGs would still exist.

We thank Y. Kannai for helpful discussions, P. Borst, S. Le Blancq, G. A. M. Cross, and M. Steinert for very helpful comments on the manuscript, and B. Sandak for technical assistance. The investigators are supported by a grant from the John D. and Catherine T. MacArthur Foundation.

1. Vickerman, K. J. (1969) *Cell Sci.* **5**, 163–193.
2. Vickerman, K. J. (1987) *Nature (London)* **273**, 613–620.
3. Cross, G. A. M. (1975) *Parasitology* **71**, 393–417.
4. Van der Ploeg, L. H. T., Valerio, D., De Lange, T., Bernards, A., Borst, P. & Grosveld, F. G. (1982) *Nucleic Acids Res.* **10**, 5905–5923.
5. Borst, P. (1986) *Annu. Rev. Biochem.* **55**, 701–732.
6. Van der Ploeg, L. H. T. (1987) *Cell* **51**, 159–161.
7. Capbern, A., Giroud, C., Baltz, T. & Mattern, P. (1977) *Exp. Parasitol.* **42**, 6–13.
8. Ross, R. & Thomson, D. (1910) *Proc. R. Soc. London Biol.* **82**, 411–415.
9. Vickerman, K. J. (1974) in *Parasites in the Immunized Host: Mechanisms of Survival*, Ciba Foundation Symposium, eds. Porter, K. & Knight, J. (Elsevier, New York), pp. 53–80.
10. Seed, J. R., Edwards, R. & Sechelski, J. (1984) *J. Protozool.* **3**, 48–53.
11. Borst, P. & Greaves, D. R. (1987) *Science* **235**, 658–667.
12. Esser, K. M. & Schoenbechler, M. J. (1985) *Science* **229**, 191–193.
13. Baltz, T., Giroud, C., Baltz, D., Roth, C., Raibaud, A. & Eisen, H. (1986) *Nature (London)* **319**, 602–604.
14. Cornelissen, A. W. C. A., Johnson, P., Kooter, J. M., Van der Ploeg, L. H. T. & Borst, P. (1985) *Cell* **41**, 825–832.
15. Lee, G.-S. M. & Van der Ploeg, L. H. T. (1987) *Mol. Cell. Biol.* **7**, 357–364.
16. Van der Ploeg, L. H. T., Shea, C., Polvere, R. & Lee, G. S. M. (1986) in *Molecular Strategies of Parasite Invasion*, UCLA Symposia on Molecular and Cellular Biology, New Series, eds. Agabian, N., Goodman, H. & Noguiera, N. (Liss, New York), Vol. 42, pp. 437–447.
17. Timmers, H. Th. M., De Lange, T., Kooter, J. M. & Borst, P. (1987) *J. Mol. Biol.* **194**, 71–90.
18. Lamont, G. S., Tucker, R. S. & Cross, G. A. M. (1986) *Parasitology* **92**, 355–367.
19. Miller, E. N. & Turner, M. J. (1981) *Parasitology* **82**, 63–80.
20. Seed, J. R. (1978) *J. Protozool.* **25**, 526–529.
21. Kosinski, R. J. (1980) *Parasitology* **80**, 343–357.
22. Herbert, W. J. (1982) *Parasite Immunol.* **4**, 209–217.
23. Doyle, J. J., Hirumi, H., Hirumi, K., Lupton, E. N. & Cross, G. A. M. (1980) *Parasitology* **80**, 359–370.
24. Myler, P., Nelson, R. G., Agabian, N. & Stuart, K. (1984) *Nature (London)* **309**, 282–284.
25. Hirumi, H., Hirumi, K., Doyle, J. J. & Cross, G. A. M. (1980) *Parasitology* **80**, 371–382.
26. Bernards, A. (1985) *Biochim. Biophys. Acta* **824**, 1–15.
27. Molyneux, D. H. & Ashford, R. W. (1983) *The Biology of Trypanosoma and Leishmania, Parasites of Man and Domestic Animals* (Taylor & Francis, New York).
28. Vickerman, K. & Barry, J. D. (1982) in *The Immunology of Parasite Infection*. eds. Cohen, S. & Warren, K. S. (Blackwell, Oxford), pp. 204–260.
29. Aline, R., Jr., MacDonald, G., Brown, J., Allison, J., Myer, P., Rothwell, V. & Stuart, K. (1985) *Nucleic Acids Res.* **13**, 3161–3177.
30. Liu, A. Y. C., Michels, P. A. M., Bernards, A. & Borst, P. (1983) *J. Mol. Biol.* **175**, 383–396.